CFD SIMULATION OF GLUCONIC ACID PRODUCTION IN A STIRRED GAS-LIQUID FERMENTER

M. Elqotbi*, L. Montastruc, S.D. Vlaev, I. Nikov

Polytech'Lille Département IAAL, ProBioGEM, Université des Sciences et Technologies de Lille, Cité Scientifique, Avenue Paul Langevin, 59655 Villeneuve d'Ascq,France;
e-mail: Iordan.Nikov@polytech-lille.fr

Abstract. Designing large-scale stirred bioreactors with performance closely matching the one achieved in lab-scale fermenters presents continuous challenge. In this contribution, dynamic modelling of the aerobic biocatalytic conversion process in viscous batch stirred tank reactor is developed. Its operation is illustrated by simulation of the interaction of fluid flow, mass transfer and reaction relevant to gluconic acid production by a strictly aerophilic *Aspergiluc niger* based on a "two-fluid" model. As a result of this simulation, the velocity fields, the local substrate, dissolved oxygen, product and biomass concentration profiles were obtained. Constant bubble size and global gas-liquid mass transfer were assumed. The algorithm employed could be used for fast evaluation procedures regarding predictions and feedback control of aerobic bioreactor performance.

Key words: Mixing, Bio-reaction, Multiphase Systems; CFD

1. INTRODUCTION

Stirred gas-liquid reactors are a major challenge in chemical industry. Numerical simulations can help to get an insight on a fermentation process where cost-saving process optimization and reactor design improvements are important. Mathematical modeling has been often the subject to empirical statistical and structural models and rarely the subject to theoretical models based on the equations of real flow. Following the work of Norman et al. [1] and Schmalzried and Reuss [2], as well as other CFD reaction engineering studies [3-5], the aim of the present work is to simulate a bioreactor productive system originating from a Navier-Stokes resolved flow field and known Contois-type kinetics.

The fermentation of gluconic acid supported by *A. niger* in a gas-liquid stirred fermenter has been targeted. The process belongs to the aerobic fermentations representing the dominant route for manufacturing of gluconic acid at present. So far two strains, i.e. *Gluconobacter oxydans* (Velizarov and Beschkov [7] and Nikov et al., [8]) and *Aspergilus niger* (Znad et al., [6]) have been studied. Both cultures are known to require high oxygen demand. The liquid in the micromyces case is a highly viscous one**.** The process is typically associated with cell growth and substrate and product inhibition. Bearing in mind that the task is computer-intensive, the method of partial solution of the simulated problem combining fluid flow and component material redistribution in the stirred vessel has been adopted.

2. NUMERICAL EXPERIMENT

2.1 The prototype system modeled

The simulation analysis was focused on bioproduction of gluconic acid by *Aspergilus niger* in a stirred gas liquid fermenter. A semi-technical scale stirred vessel with a standard geometry D=T/3, tank diameter T = 0.4 m and aspect ratio H/T = 1, where D is impeller diameter and H is liquid height, was assumed. The configuration was chosen to be close to the conditions in conventional industrial vessels intended for gas-liquid processing.

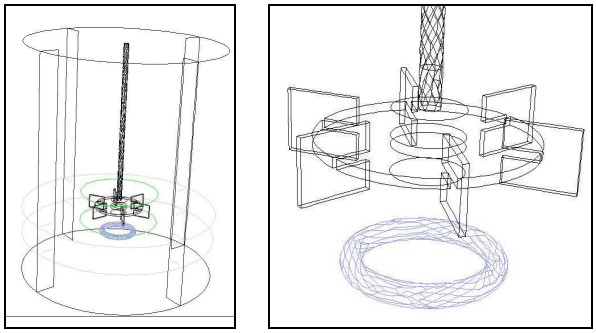

Fig. 1 Computer rendition of the bioreactor set-up

2.2 Model equations and assumptions

The model equations employed governing the flow and the material transfer are presented in Table 1. Index *L* indicates the liquid (substrate) continuous phase and index *G* stands for the oxygen delivering gas dispersed phase. The four components dispersed in the liquid are cell biomass *X*, glucose substrate *S*, dissolved oxygen O_d and gluconic acid product *P*.

Table 1 Basic equations governing momentum and material transport in the case considered

Momentum / Reaction Stages	Equations
Two-phase flow (aqueous continuous phase and oxygen containing gas disperse phase)	$\frac{\partial \alpha_L \rho_L}{\partial t} + div\left(\alpha_L \rho_L \vec{v}_L\right) = 0$ (1)
	$\frac{\partial \alpha_G \rho_G}{\partial t} + div\left(\alpha_G \rho_G \vec{v}_G\right) = 0$ with $\alpha_L + \alpha_G = 1$ (2)
	$\frac{\partial}{\partial t}\left(\alpha_L \rho_L \vec{v}_L\right) + div\left(\alpha_L \rho_L \vec{v}_L \otimes \vec{v}_L\right) = -\alpha_L \overrightarrow{grad}\, p + \alpha_L \rho_L \vec{g} + div\overline{\overline{T}}_L$ (3)
	$\frac{\partial}{\partial t}\left(\alpha_G \rho_G \vec{v}_G\right) + div\left(\alpha_G \rho_G \vec{v}_G \otimes \vec{v}_G\right) = -\alpha_G \overrightarrow{grad}\, p + \alpha_G \rho_G \vec{g} + \alpha_G \rho_G \overrightarrow{f_{G_{lift}}} + div\overline{\overline{T}}_G$ (4)
Mass balance (to be solved for each of the reacting components)	$\frac{\partial}{\partial t}\left(\alpha_L \rho_L c\right) + div\left(\alpha_L \rho_L c v_L\right) = r_c$, where c = *X, S, O_d, P* *(5-8)*
Mass transfer	$r_{O_d} = r_{(O2_{bubble} \rightarrow O2_{dissolved})} = (k_L a)_{O2}(O_d^* - O_d)$ (9)

The kinetic data of Znad et al. (2003) were used and the gluconic acid fermentation process was described by the following Contois-type model [6]; (different yield/consumption ratios are considered for different components in the liquid phase):

$$r_X = \frac{dX}{dt} = \mu X \tag{10}$$

$$r_S = \frac{dS}{dt} = -\gamma \frac{dX}{dt} - \lambda X \qquad with \quad \gamma = 2{,}1768 \; and \; \lambda = 0{,}2937\, h^{-1} \tag{11}$$

$$r_{O_d} = \frac{dO_d}{dt} = k_L a(C^*_{O_d} - C_{O_d}) - \delta \frac{dX}{dt} - \phi X \qquad with \quad \delta = 0{,}2724 \; and \; \phi = 0{,}0425\, h^{-1} \tag{12}$$

$$r_P = \frac{dP}{dt} = \alpha \frac{dX}{dt} + \beta X \qquad with \quad \alpha = 2{,}5800 \; and \; \beta = 0{,}1704\, h^{-1} \tag{13}$$

with

$$\mu = \mu_m \frac{S}{K_S X + S} \frac{O_d}{K_{O_d} X + O_d} \qquad with \quad \mu_m = 0.361\, h^{-1} \quad \text{acc. to the model of CONTOIS} \tag{14}$$

The following major assumptions are valid: (1) steady flow field not affected by gas-liquid mass transfer and reaction, (2) mass transfer performing under a constant specific rate coefficient condition, i.e. $k_L a$=63 h^{-1}, (3) diffusion among the four components in the liquid is negligible, (4) near-laminar flow or Re<10^3 , (5) oxygen transfer at condition of constant bubble size of tiny bubbles ca. 1 mm, (6) gas is introduced by porous ring distributor at 8 dm^3/min.

3.3 Numerical procedure and platform

The computational model contained 3D-grids with a total of up to 320000 mixed tetrahedral and triangular cells. The mesh of the tank was unstructured, as formulated by MIXSIM 2.0. Grid refinement around the gas sparger was used. Impeller motion was modeled using the "inner-outer" solution approach and a single reference frame model (SRF). Referring to the flow field solution, the number of iterations was ca. 6000 with a second order upwind for obtaining steady state flow. The number of iterations in the other three stages was a function of the time step size Δt, e.g. 21000 iterations were carried out at $\Delta t = 10s$; the biological reaction delay was 60h.

In order to reduce the dimension of the largely intensive computing task, the simulation was carried out separately for the flow and the reactive conditions. FLUENT 6 code version 18 [9] was used.

The heterogeneous reaction system was described as a "two-fluid" model. The "Euler-Euler" approach was utilized.

Referring to the reaction phase, the set of differential equations comprising the detailed mass balances of the cells, the glucose, the product, and the dissolved oxygen, and the gas phase oxygen in the bulk were solved simultaneously. The kinetic parameters values used were taken both from the authors' own studies and from the literature [6, 8]. The ratios r_X, r_{O_d}, r_S and r_P were implanted as user defined functions (UDF). The time courses of bulk concentrations of substrates, oxygen, products and biomass with a product inhibition term have been resolved.

The computational platform comprised a PC 2.4 Ghz and 1 Gb RAM. In order to reduce the time-scale of the computer-intensive task, partial computer analysis in four stages of

simulation was adopted (see Table 2): stage **1** of gas-liquid fluid flow and steady-state achievement, stage **2** of liquid-phase oxygen saturation, stage **3** of culture injection and spread, and stage **4** – the biological reaction.

Table 2 Time-table of stage evolutions

Stage	1	2	3	4
Operation	Two-phase steady state	DO saturation	Cell sample injection and spread	Biological reaction
Number of iterations/ time delay	≈6000 iterations	≈20 min	a few iterations ≈ a few seconds	60h ≈ 21000 iterations

3. RESULTS AND DISCUSSION

In parallel to the four stages above, the following results were obtained.

Initially, the flow equation system was resolved and a steady flow field was obtained. The field of the local velocity vector obtained for the liquid and the gas phase is illustrated in Figs. 2(a) and 2(b), respectively.

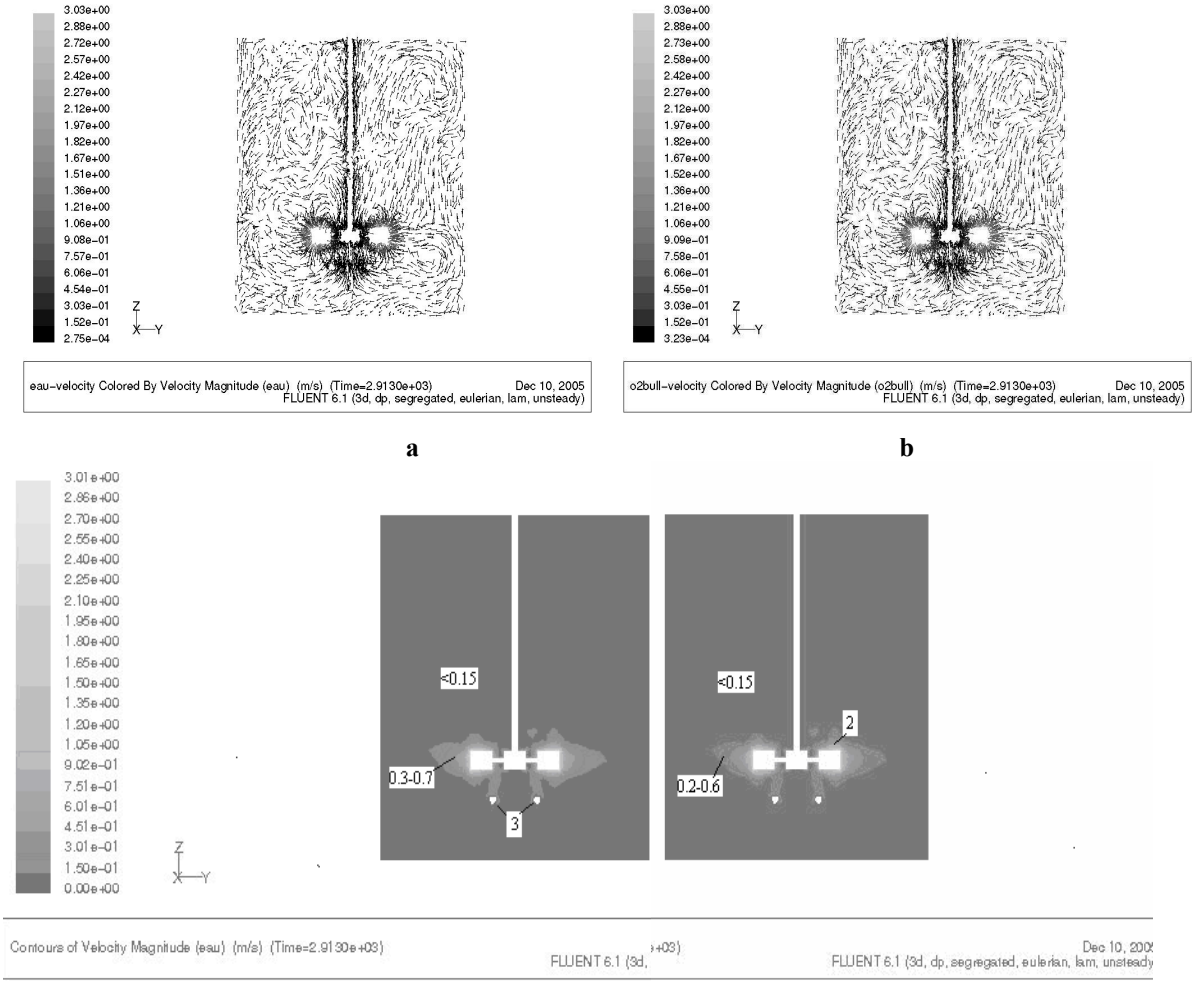

Fig.2 Fields of local velocity vectors and contours of velocity magnitude for the liquid (a) and the gas(b) phases.

It should be noted that the general type of radial primary discharge in the impeller zone coupled with secondary subsurface circulation in the sub-surface area observed for Rushton

turbines is confirmed. At this stage, the liquid phase component concentrations were 150g/ dm^3 of substrate, 4.5 mg/dm^3 of dissolved oxygen, 1 mg/ dm^3 of product and 0 mg/ dm^3 of culture.

Further, the procedure of oxygen saturation has been switched on and oxygen transfer has been simulated, as registered by volume-weighted average dissolved oxygen concentration time-course in Fig. 3(a). The dissolved oxygen (DO) concentration increased from 4.5 mg/L to ca. 8 mg/dm^3. At the end of this stage, complete mixing and uniformity of DO concentration was ensured, as registered in Fig. 3(b).

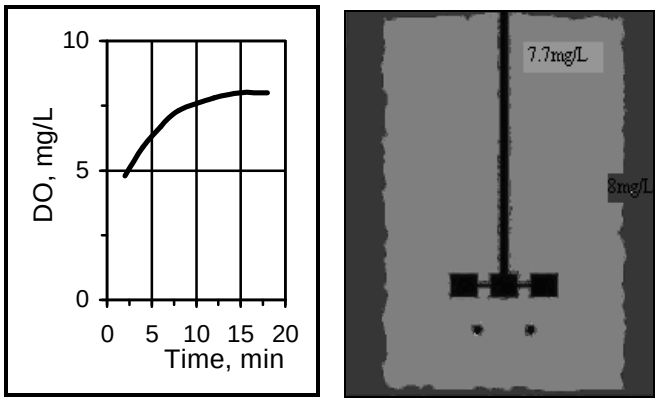

a *b*

Fig. 3 Dissolved oxygen saturation time-course (a) and contour plot (b).

Then, the culture has been injected in the medium near the impeller at an initial mean concentration of 0.2 g/dm^3, as illustrated in Fig. 4(a) and has been homogenized almost completely, as illustrated in Fig. 4(b)

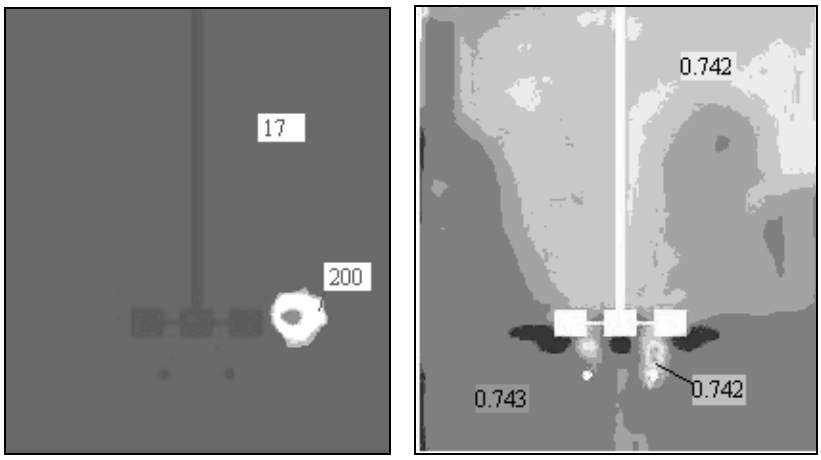

a

b

Fig.4 Culture injection (a) and spread (b) in the bioreactor (g/L)

The biochemical reaction process is illustrated in Fig.5 following the fourth stage and the end of fermentation. Both cell growth and gluconic acid accumulations are illustrated by time-

courses in Figs. 5(b) and 5(d). The production process is accompanied by substrate and dissolved oxygen uptake illustrated by the curves in Figs. 5(a) and 5(c), respectively. The

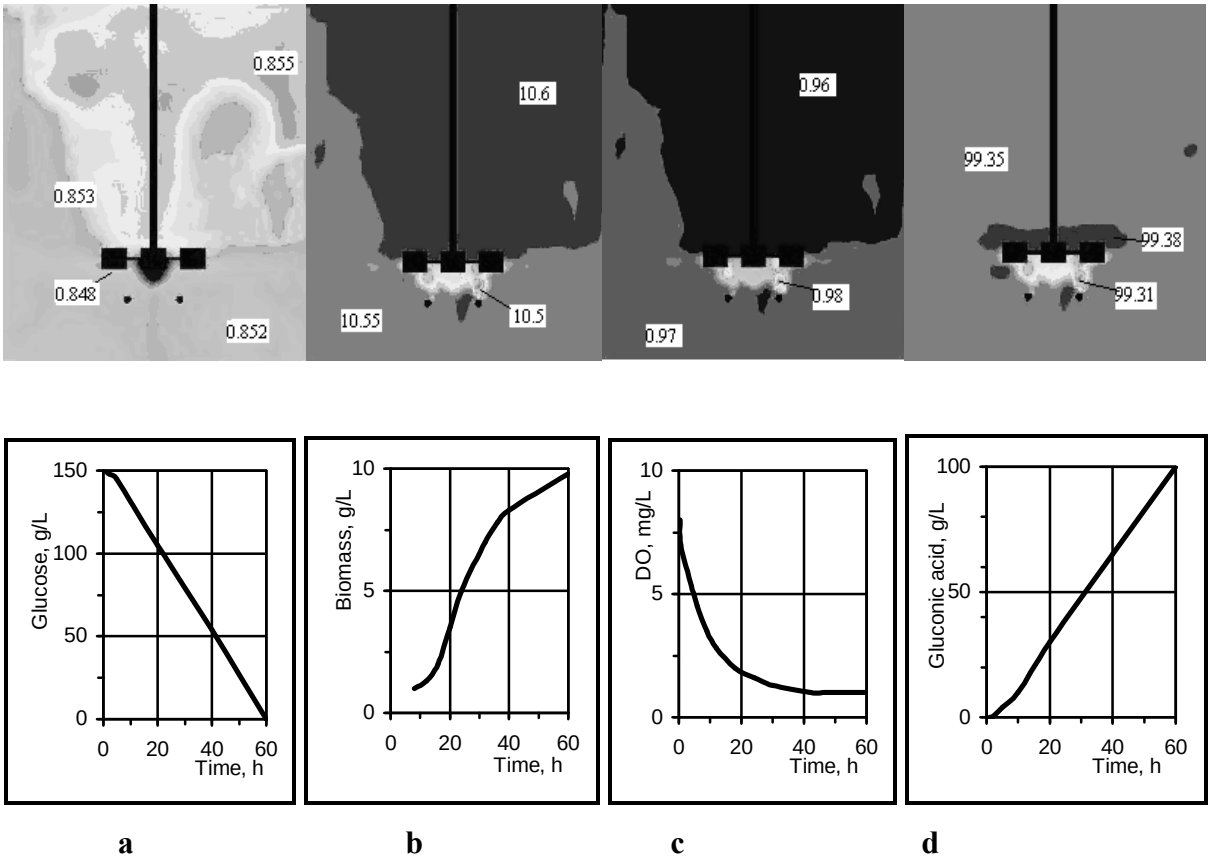

Fig.5 Components' spatial distribution and the relevant time-courses following 60 h fermentation for the glucose substrate (a) the biomass (b), the dissolved oxygen (c) and the gluconic acid (d)

simulation terminated at zero substrate concentration that was reached in the 60th hour. The final component distributions are presented by the contour plots in the figure. Evidently from these plots, all components were completely mixed and showed no spatial concentration gradients, e.g. the differences were within or even less than 10^{-1} g/dm^3.

The simulation data in Figs. 5(a)-(d) were compared with laboratory results obtained for the same system by Znad et al (2004)[6]. These authors used a mechanically stirred bioreactor in two versions volumes of 2 and 5 dm^3 and recommended using the kinetic model of COntois for the reaction. In the reference experiment, the bioreaction has been stopped following 58 h fermentation. Znad et al. reported oxygen concentrations profiles between.6 and1 mg/dm^3. These data compare well with our delivered range, e.g. 6.5 mg/dm^3 through 1 mg/dm^3. The gluconic acid production in both cases varied between zero and 70-80 g/dm^3. The biomass and substrate concentrations were also compared and lied within compatible ranges, e.g. between zero and 8-10 d/ dm^3 and between 150 g/dm^3 and 40 g/dm^3, respectively.

It should be noted that while varying the global $k_L a$ value in the range 45-80 h^{-1}, the $k_L a$ effect on the kinetic parameters remained negligible.

4. CONCLUSION

An advanced analysis of a bioreactor system involving a Navier-Stokes based model has been accomplished. The model allows a more realistic impeller induced flow image to be combined with the real Contois bioreaction kinetics. The general time-course of gluconic acid production supported by *Aspegilus niger* in real time of a 60 hour-fermentation run has been simulated at kinetic conditions proposed by Znad et al.(2004). The simulation is based on the approach of separate solution of the mixing flow field and the mass transfer and reaction based on the assumption of a stationary flow field that is not affected by mass transfer and reaction. Preliminary tests of the results against real data by reference show good qualitative prediction potentials of the model. As a CFD-based bioreactor solution, the simulation requires increased computational effort, however, renders a multiple output versatile for further post-processing analyses and optimization avoiding the enormous effort, time and resources required for experimental work.

NOMENCLATURE

D	impeller diameter, m
N	impeller speed, s^{-1}
Re	impeller Reynolds number, $\rho ND^2/\mu$
T	tank diameter, m
α	volume fraction in Eqs.(1)-(8)
ρ	density ($kg.m^{-3}$)
v	velocity ($m.s^{-1}$)
p	pressure (Pa)
g	gravity
α_1	growth-associated product formation coefficient in Eq.(13).
β	non growth-associated product formation coefficient, h^{-1}
γ	growth-associated parameter of substrate uptake in (Eq. 11); substrate mass consumed per biomass mass grown
δ	oxygen uptake parameter in Eq.(12); oxygen mass consumed per biomass mass grown
λ	non-growth-associated substrate uptake parameter in Eq.(11); substrate mass consumed per biomass mass grown, h^{-1}
μ	specific growth rate, h^{-1}
μ_m	maximum specific growth rate, h^{-1}
ϕ	oxygen uptake parameter in Eq.(12); oxygen mass consumed per biomass mass grown per hour
L	stands for liquid
G	indicates gas
CFD	computational fluid dynamics
DO	dissolved oxygen
GA	gluconic acid
UDF	user defined function

REFERENCES

1. Norman H., Morud K., Hjertager B.H., Trägärd C., Larson G., Enfors S.O., 1993. "CFD modelling and verification of flow and conversion in a 1 m^3 bioreactor", In: Nienow, A.W. (Eds.), *Proc. 3d Int. Conf. on Bioreactor and Bioprocess Fluid Dynamics*, MEP/BHR Group, Cranfield, pp. 241-258.
2. Scmalzriedt S., Reuss M., 1997. "Application of CFD to simulations of mixing and biotechnical conversion process in stirred tank bioreactors", *Récent Progrès en Génie des Procédés,* **11**(S1), 171-178.
3. Davidson K.M., Sushil S., Eggleton C. D., Marten M. R., 2003. "Using CFD software to estimate circulation time distribution", *Biotechnol. Prog.*, **19**, 1480-1486.
4. Hristov H.V., Mann R., Lossev V., Vlaev S.D., 2004. "A simplified CFD for three-dimensional analysis of fluid mixing, mass transfer and bioreaction in a fermenter equipped with triple novel geometry impellers", *Food and Bioproduct Processing*, **82**, 21-34.
5. Rudniak L., Machniiewski, P.M., Milewska, A., Molga, E., 2004."CFD modeling of stirred tank chemical reactor: homogenous and heterogeneous reaction systems", *Chem. Eng. Sci*., **59,** 5233-5239.
6. Znad H.,Blazej M., Bales V., Markos J., 2004. "A kinetic model for gluconic acid production by *Aspergillus niger*", *Chem. Pap*., **58**(1), 23-28.
7. Velizarov S., Beschkov V., 1998. "Biotransformation of glucose to free gluconic acid by *Gluconobacter oxydans*: substrate and product inhibition situations", *Proc. Biochem*., **33** (5), 527-534.
8. Nikov I., Doneva T., Vassilieff, C., 1998." Catalytic and biocatalytic oxidation of glucose to gluconic acid in a modified three-phase reactor*", Proc. 2nd Int. Symp. on Catalysis in Multiphase Reactors* (Toulouse-France, 16-18 March) pp. 383.
9. FLUENT User's Guide, 1998, FLUENT Inc., New Hempshire, 1998.